Comparison of Adsorption Properties of Activated Carbons with Different Crops Residues as Precursors for Gold Cyanide Recovery: An Iranian Gold Industry Guide

Salehi, Ehsan*[+]; Yarali, Majid; Ebadi Amooghin, Abtin
Department of Chemical Engineering, Faculty of Engineering, Arak University,
P.O. Box 38156-8-8349 Arak, I.R. IRAN

ABSTRACT: *Adsorption of gold cyanide on three types of Activated Carbons (ACs) has been investigated in batch and column adsorption conditions. Applied ACs have been derived from different crops precursors i.e., coconut shell (CAC), peach stone (PAC) and walnut shell (WAC). As peach stone and walnut shell are abundant agricultural residues in Iran, the activated carbons produced from these precursors are economically preferable for the gold recovery process. The ACs were characterized using FTIR, SEM, BET, and Wet-Bed Compaction Hardness analyses. Batch equilibrium adsorption data was analyzed using the Langmuir, Freundlich, Temkin, and Dubinin–Radushkevich isotherm models. Freundlich isotherm was in better agreement with the equilibrium data and the maximum adsorption capacity (40.8 mg/g) was tabulated for CAC. Adsorption kinetics was also modeled using pseudo-first order, pseudo-second order, and intraparticle diffusion models. The PAC recorded the highest removal rate in the light of better agreement of the pseudo second order model. Fixed-bed column experiments were carried out at different initial gold concentrations (30, 50 mg/L) to determine the characteristics of the breakthrough curves. The maximum bed capacity (37.55 mg/g) was obtained for CAC. Three dynamic adsorption models including, Thomas, Yoon–Nelson, and Adam–Bohart, were applied to describe the breakthrough curves. Both Thomas and Yoon–Nelson models were in appropriate agreement with the experimental column adsorption data. This research introduces peach stone as a promising precursor considering availability, technical features, and economical aspects for the production of AC for gold recovery from cyanide leach solutions. Results are also conductive for gold mining industries to select the appropriate activated carbon.*

KEYWORDS: *Adsorption; Pregnant liquor; Gold cyanide; Fixed-bed column; Breakthrough curves.*

INTRODUCTION

Gold is a valuable metal which plays an impressive role in the world economic affairs due to the increasing demand for gold usage in jewelry, electronics, and medicine industries. Typically, gold is not directly recovered. Extraction of gold in industrial scale involves two important steps: reducing the size of the ore rocks

** To whom correspondence should be addressed.*
+ E-mail: e-salehi@araku.ac.ir ; ehsan1salehi@gmail.com
1021-9986/2020/3/213-229 17/$/6.07

(physical processing), separating gold from other components comprising the ore rocks (chemical processing). Among chemical treatments, cyanidation is the most commonly used method for gold leaching from its ore [1-3]. The chemical reaction is as follows [2]:

$$4Au_{(s)} + 8CN^-_{(aq)} + O_{2(g)} + 2H_2O_{(l)} \rightarrow 4Au(CN)^-_{2(aq)} + 4OH^-_{(aq)} \quad (1)$$

To extract gold, the gold-cyanide complex ($Au(CN)^-_{2(aq)}$) is adsorbed on the large surface area of the activated carbon followed by selecting an appropriate technique from a variety of recovery technologies. Among conventional methods for the extraction of gold complexes from cyanide leach solution, adsorption onto activated carbon is the most prevalent process. Carbon in Pulp (CIP), Carbon in Column (CIC), and Carbon in Leach (CIL) are three common AC-based technologies for the gold cyanide recovery [4-6]; however, the CIP is the most prevalent technique [7, 8]. The other important process for gold recovery is the Merrill-Crowe zinc precipitation. The advantages of CIP over zinc precipitation method include not only more efficient gold recovery but also lower operating and capital costs [9].

Gold production process includes two important unit-operations as "activated carbon adsorption" and "elution". The loaded ACs is leached out after adsorption and gold is recovered. The gold-rich eluant obtained from the elution stage contains the extracted gold and is called the pregnant liquor.

Activated carbon is a highly porous organic material composed of a series of graphitic plates, which are interconnected by carbon-carbon bonds. This structure creates high porosity and gives an extensive internal surface area for adsorption of gold. Activated carbon can be derived from a variety of different precursors including coal, wood, agricultural wastes and inorganic materials like, lignite which are the primary materials used to make commercial-scale activated carbons. Moreover, agricultural residues such as hard nut shells (macadamia, almond, pecan, walnut and hazelnut) and fruit stones (apricot, cherry and peach stones) [10-13], are also economically favorable alternative sources for activated carbon production. The starting material (precursor) can greatly affect the activated carbon characteristics such as pore size, pore distribution, reactive sites type and density and mechanical hardness. Coconut shell is the most prevalent precursor for the ACs applied in the gold recovery industry because of its high adsorption capacity, suitable uptake rate, and high physicochemical stability against abrasion and compaction in CIC unit [7, 13]. To maximize the gold loading on the activated carbon which affects the overall gold production yield, it is important to select a high quality activated carbon with appropriate chemical and physical properties.

Many studies have concentrated on the adsorption of complex $Au(CN)^-_{2(aq)}$ onto activated carbons made from raw materials such as agricultural wastes and modified ACs [13, 14-19]. The potential of our country, Iran, for producing ACs from abundant vernacular raw materials such as peach stone and walnut shell is an important issue which cannot be ignored by the Iranian gold mining industries. Accordingly, techno-economic feasibility of replacing CAC with the more available (due to the abundant sources) WAC and PAC needs to be investigated.

To the authors' knowledge, a few research focused on the gold adsorption from the Au-pregnant liquor on the ACs with different starting materials are reported in the literature. This study is aimed at comprehensive batch and dynamic adsorption investigation of three types of activated carbons (CAC, WAC, and PAC) applied in gold cyanide recovery. Isothermal, kinetics and fixed-bed column properties of the AC/gold-cyanide adsorption system have been thoroughly tackled. Various chemical and morphological analyses were also performed to characterize and understand the chemical/structural differences among the ACs. The obtained results would be conductive to the mining industries to select the best AC alternative regarding both economic and technical viewpoints for the gold recovery from the gold-cyanide rich liquor.

EXPERIMENTAL SECTION

Materials

Coconut-shell based granular Activated Carbon (CAC) which is currently used in the process line (Zar Kuh mining company, Qorveh, Kurdistan, Iran) provided by Haycarb Company, Sri Lanka. Peach-core based granular Activated Carbon (PAC) and Walnut-shell based granular Activated Carbon (WAC) gifted by the Part Chemical Company, Hamedan, Iran, were also applied in order to be compared

Table 1: Physical Characteristics of applied ACs.

Parameter	Activated Carbon		
	CAC	PAC	WAC
Mesh (US standard sieve size)	6×12	6×12	6×12
Attrition hardness (%)	99	95	85
Density(kg/m^3)	560	500	400
Ash content (%)	1.8	3	7
Moisture content (%)	2	<10	5
S_{BET} (m^2/g)	1232	1180	1120
WBCH* (cm)	1.3 ± 0.05	2.0 ± 0.05	3.2 ± 0.05

**Bed height lost at initial bed mass of 10 g and external mass of 30 kg after 48 h.*

with CAC for the adsorption of $Au(CN)_{2(aq)}^{-}$. The specifications of the ACs are listed in Table 1. Sodium cyanide (NaCN), sodium hydroxide (NaOH), Silver nitrate ($AgNO_3$), and potassium iodide (KI) were obtained from Merck. The $Au(CN)_{2(aq)}^{-}$ solution was directly supplied from the pregnant liquor discharged from the CIC unit. All the other reagents were of analytical grade and used as received.

Characterization

Various tests were employed to determine the physical and chemical properties of the ACs. The BET surface areas of the three ACs were calculated according to physical adsorption/desorption of nitrogen at 77 K using Gemini VII 2390 Surface Area Analyzer. The scanning electron microscope (SEM, Philips XL30 model) was used to examine the microstructure of the adsorbents. The adsorbents were also analyzed using ABB Bomem (model: MB-104) FTIR spectrometer in order to identify the functional groups of the ACs. A novel compaction resistance test namely, wet-bed compaction hardness was designed and performed to compare the mechanical resistance of the ACs in column mode.

Gold Recovery Experiments

$Au(CN)_{2(aq)}^{-}$ Solution

The $Au(CN)_{2(aq)}^{-}$ solution was directly obtained from the pregnant liquor discharged from the desorption stage of the actual process. For each adsorption test, this solution was diluted by water to prepare desired sample solutions with distinct gold concentrations. Next step was adjusting the cyanide concentration and the pH of the sample solutions to those of the actual process line. The free cyanide (CN^-) was measured through titration with silver nitrate ($AgNO_3$), using potassium iodide (KI) as the indicator, and adjusted to the desired value by adding predetermined amount of the NaCN. pH of all the sample solutions were adjusted to 11 by adding 1.25 M NaOH solution.

Static equilibrium adsorption

Batch adsorption tests were carried out by introducing 3 g of adsorbent in 2.5 l bottles containing 1 l gold solution with various initial concentrations (10–200 mg/l) at room temperature. The bottles were sealed and roll-shacked at constant rotation speed of 60 rpm for 24 h to reach the equilibrium. Afterwards, the solution was filtered with common filter papers and the final concentration of the supernatant solution was measured using atomic absorption spectrophotometer (Varian SpectrAA220). The amount of gold adsorbed per unit mass of adsorbent (q_e) can be determined by using the following equation:

$$q_e = \frac{(C_0 - C_e)V}{m} \quad (2)$$

where C_e is the equilibrium concentration of gold (mg/l) in the supernatant.

Equilibrium adsorption data were analyzed using four widely-used isotherms including Langmuir Eq. (3), Freundlich Eq. (4) and two more models including Temkin, and Dubinin–Redushkevich (D-R).

$$q_e = \frac{q_{max} k_L C_e}{1 + k_L C_e} \quad (3)$$

$$q_e = k_f C_e^{1/n} \quad (4)$$

Where q_{max} is the maximum adsorption capacity, k_L (l/mg) is the Langmuir constant related to the free energy of adsorption. k_f ((mg/g) (l/mg)$^{1/n}$) is the Freundlich sorption constant and 1/n is related to the adsorption intensity. To measure the adsorption favorability, a dimensionless constant named, separation factor (R_L), is defined by the following equation:

$$R_L = \frac{1}{1 + k_L C_0} \quad (5)$$

For a favorable adsorption, the amount of R_L should be between zero and 1.

The Temkin isotherm is given by the following equation:

$$q_e = \frac{RT}{b_T} \mathrm{Ln}\left(A C_e\right) \quad (6)$$

Where A is the Temkin isotherm constant (l/g), b_T is the Temkin constant related to adsorption heat (J/mol), R is the gas universal constant (8.314 J/mol K) and T is the absolute temperature (K).

The Dubinin–Radushkevich (D-R) isotherm is presented by Eq. (7) to (9):

$$q_e = q_{max} \exp\left(-B\varepsilon^2\right) \quad q_t \quad (7)$$

$$\varepsilon = RT\mathrm{Ln}\left(1 + \frac{1}{C_e}\right) \quad (8)$$

$$E = \frac{1}{\sqrt{2B}} \quad (9)$$

where ε is the Polanyi potential, E is the free energy of adsorption (J/mol) and B is the constant related to the sorption energy (mol^2/J^2).

It is worth mentioning that the equilibrium, kinetic and subsequently the dynamic constants were calculated through non-linear regression using Curve Fitting Toolbox of MATLAB (R2009a) software.

Kinetics

Adsorption kinetic tests were conducted to evaluate the gold adsorption rate and mechanism. Batch adsorption tests were performed using rolling bottle shaking method in 2.5 l bottles containing 1 l gold cyanide solution and 3g of the adsorbent at room temperature (25 ±2 ◦C). The bottles were sealed and rolled at constant rotation speed of 60 rpm for 6 h. During the operation, gold solution samples were being taken in predetermined time intervals. The content of the bottles were filtered as before and gold concentration of the filtrate was analyzed by the atomic absorption spectrophotometer. The gold uptake at time t was calculated by the following equation:

$$q_t = \frac{\left(C_0 - C_t\right)V}{m} \quad (10)$$

Where q_t is the amount of solute adsorbed per unit mass of the adsorbent (mg/g), C_0 and C_t are the initial and time-dependent gold concentrations in the $Au(CN)_{2(aq)}^-$ solution (mg/l), respectively. V (l) is the volume of the $Au(CN)_{2(aq)}^-$ sample solution, and m is the adsorbent dry mass (g).

In present work, pseudo-first-order Eq. (11), pseudo-second-order Eq. (12) and intraparticle diffusion (Eq. (13)), models were employed to describe the kinetic of the adsorption process:

$$\log\left(q_e - q_t\right) = \log q_e - \frac{k_1 t}{2.303} \quad (11)$$

$$\frac{1}{q_t} = \frac{1}{k_2 q_e^2} + \frac{2}{q_e} \quad (12)$$

$$q_t = k_p \cdot t^{0.5} \quad (13)$$

where q_e and q_t are the amount of solute adsorbed per unit mass of adsorbent (mg/g) at equilibrium and at time t, respectively. k_1 (min^{-1}), k_2 (g/mg min) and k_p (mg/g min$^{0.5}$) are adsorption rate constants.

It is worthy of notice that all the experiments (including isothermal, kinetics and column tests) have been randomly replicated in triplicate and the maximum deviation from the average values was less than 5%.

Validity of static and dynamic adsorption models

In addition to the prevalently used correlation coefficient (R^2), the hybrid error function (HYBRID) was also used to measure the goodness of the fits. The HYBRID equation can be expressed as:

$$\text{HYBRID} = \frac{100}{N-p}\sum_{i=1}^{N}\left[\frac{\left(q_{ei}^{exp}-q_{ei}^{cal}\right)^2}{q_{ei}^{exp}}\right] \quad (14)$$

Where q_{ei}^{exp} (mg/g) is the observed adsorption amount for the i-th experiment, q_{ei}^{cal} is the adsorption amount estimated by the isotherm model, N is the number of the observations and p is the number of the parameters used in the model. The smaller values of the HYBRID function reflects the appropriateness of the applied model. For the kinetics and fixed bed column studies, q_{ei} is replaced by q_{ti} and C_{ti}, respectively.

Fixed-bed column

Setup

A plastic cylinder with an internal diameter of 1.5 cm and the length of 19 cm was used as the fixed-bed column. A thin layer of glass wool was placed at the bottom of the column to prevent stream channeling and blockage of the plastic tube by the adsorbents during the process. 7g of fresh AC was loaded in the column for each run. The $Au(CN)_{2(aq)}^{-}$ solution of known concentration (30, 50 mg/L) was continuously fed upward into the column at the constant flow rate of 20 mL/min using a roller clamp tubing system. This system consists of a plastic tube and a roller clamp. Plastic tube connects the reservoir of the gold solution to the bottom of the column and the roller clamp was used to control the flow rate of the solution. The $Au(CN)_2^-$ solution samples were collected from the outlet of the column at pre-determined time intervals and analyzed for gold concentration using atomic absorption spectrophotometer (Varian SpectrAA220).

Mathematical framework

The analysis of the breakthrough curves is an appropriate way to evaluate the performance of a typical fixed-bed column. Mechanism of adsorption process, flow velocity and feed concentration are important factors obtained through the breakthrough curves. Commonly, the breakthrough curve is defined as the ratio of the outlet gold concentration to the feed concentration (C_{eff} /C_o) as a function of time or volume of the effluent, V_{eff} (mL), as shown by the following equation:

$$V_{ff} = Qt_{total} \quad (15)$$

where Q and t_{total} represent the volumetric flow rate (mL/min) and time (min), respectively. The point where C_{eff} /C_o=0.05 is defined as breakthrough time (t_b) while exhaustion time (t_e) corresponds to C_{eff} /C_o=0.95. The amount of the total gold adsorbed, q_{total} (mg), by the column can be obtained from the area under the breakthrough curve using the following equation:

$$q_{total} = \frac{QA_r}{1000} = \frac{Q}{1000}\int_{t=0}^{t=total} C_{ad}dt = \int_{t=0}^{t=total}\left(C_0 - C_{eff}\right)dt \quad (16)$$

The total amount of gold received by the column, m_{total} (mg), is represented as below:

$$m_{total} = \frac{C_0 Qt_{total}}{1000} \quad (17)$$

The equilibrium gold uptake or in other word, the maximum capacity of the column, q_e (mg/g), can be written as:

$$q_{eq} = \frac{q_{total}}{m} \quad (18)$$

where m (g) is the dry mass of the adsorbent loaded in the column. At equilibrium, unabsorbed gold concentration in the dynamic adsorption system is calculated as follows:

$$c_{eq} = \frac{m_{total} - q_{total}}{V_{eff}} \times 1000 \quad (19)$$

The total removal percentage (Y) of gold is also evaluated as given by Eq. (19):

$$Y = \frac{q_{total}}{m_{total}} \times 100 \quad (20)$$

Modeling of column data

Thomas model

This breakthrough model estimates the adsorption capacity of the bed. Constant void fraction of the column, negligible radial and axial dispersion in the bed, isobaric and isothermal operating conditions, no signs of resistance against intraparticle and external diffusion are some of the basic assumptions of this model [20]. The linearized form of the Thomas model is given by:

$$\ln\left(\frac{C_0}{C_t} - 1\right) = \frac{k_{Th} q_0 m}{Q} - k_{Th} C_0 t \quad (21)$$

Where k_{Th} (mL/min.mg) is the Thomas rate constant, q_0 (mg/g) is the adsorption capacity of the column, C_t (mg/L) is the effluent gold concentration at time t and at last t is flow time (min).

Yoon-Nelson model

The Yoon–Nelson model has been developed based on the assumption that the decrease in the probability of each adsorbate is proportional to the probability of its adsorption and breakthrough on the adsorbent [21, 22]. Simplicity and fewer requirements to the detailed column data are some advantages of this model [23].The linearized form of the Yoon–Nelson model for a single component system is represented by:

$$\ln\frac{C_t}{C_0 - C_t} = k_{YN}t - \tau k_{YN} \quad (22)$$

where k_{YN} (min^{-1}) and τ (min) are the Yoon-Nelson rate constant and the time required for 50% adsorbate breakthrough, respectively.

Adams-Bohart model

Adams-Bohart model is based on the theory of surface reaction and assumes that equilibrium does not reach immediately [24]. This model is proper for the description of the initial part of the breakthrough curve [25]. The Adams-Bohart model is expressed as follows:

$$\ln\frac{C_t}{C_0} = k_{AB}C_0 t - k_{AB}N_0\frac{Z}{U_0} \quad (23)$$

where k_{AB} (l/mg ·min) is the Adam–Bohart kinetic constant, U_0 (cm/min) is the linear velocity calculated by dividing the flow rate by the column section area, Z (cm) is the bed depth of the column and N_0 (mg/L) is the saturation concentration.

RESULTS AND DISCUSSION

Characterization

FT-IR

Fig. 1(a) presents the FTIR spectra for CAC before and after adsorption of gold. In the case of unloaded CAC, three major intense peaks around 3428, 1383 and 1083 cm^{-1} besides a moderate band at 1616 cm^{-1} are related to O-H stretching, O-H bending, C–O–C stretching and C=C stretching vibrations, respectively [26]. Considering these peaks, the main functional groups on the surface of the CAC can be expressed as hydroxyl and carboxylic anhydride groups. Figs. 1(b) and 1(c) show the FT-IR spectra of loaded and unloaded PAC and WAC, respectively. For both unloaded ACs, the adsorption peaks around 3100-3500 cm^{-1} region are attributed to OH stretching band of hydroxyl groups, the peak at 1125 cm^{-1} can be ascribed to O-H (carboxylic) or C-O (phenolic) and furthermore, the absorption bands at 1380-1700 cm^{-1} region are ascribed to carbonyl (C=O, stretching vibration) and aromatic (CH) groups [27]. For unloaded PAC the band at 2360 cm^{-1} indicates the existence of C≡N in the nitrogen containing functional groups.

Most of the spectral analyses used to identify the mechanism of gold adsorption, have resulted in reduction of the ionic gold to the elemental gold [28, 29]. For all the Au-loaded ACs in Fig. 1, shift of specific FT-IR peaks signify the interactions between the solute and the functional groups on the surface of the adsorbents. Similar observation is obtained for the IR spectra after gold adsorption elsewhere [28, 29]. For example in Fig. 1(a), O-H stretching at 3428 shifts to 3447 cm^{-1} and C=C stretching at 1616 changes to1630 cm^{-1}. The peaks at 1383 and 1083 cm^{-1} shifts to 1401 and 1108, respectively. In addition to this, for Au-loaded CAC and PAC, the increase in the intensity of the bands at 1558 cm^{-1} and 1586 cm^{-1} can be attributed to the oxidation of hydroxyl groups on the surface of the ACs to the carbonyl groups as shown below:

$$R - OH \rightarrow R = O + H^+ + e^- \quad (24)$$

Thus, OH stretching vibration of hydroxyl groups plays an important role in gold adsorption. As can be seen in Fig. 1, the intensity of OH stretching vibration for various adsorbents before adsorption follows this order: CAC > PAC > WAC

The other important difference among the three ACs before adsorption appears at 1000-1130 cm^{-1} region. The intensity of this band which can be ascribed to Si-O stretching vibration of mineral elements in the carbons [30], obeys the following order: WAC > PAC > CAC. This result is in agreement with the amount of ash content presented in the ACs structure, as depicted in Table 1. Ash content reduces the adsorption capacity of the ACs.

The increase in the transmittance intensity of the gold-loaded ACs is the consequence of oxidation of functional groups during reduction of gold- cyanide complex ions and appearance of R=O stretching band [28].

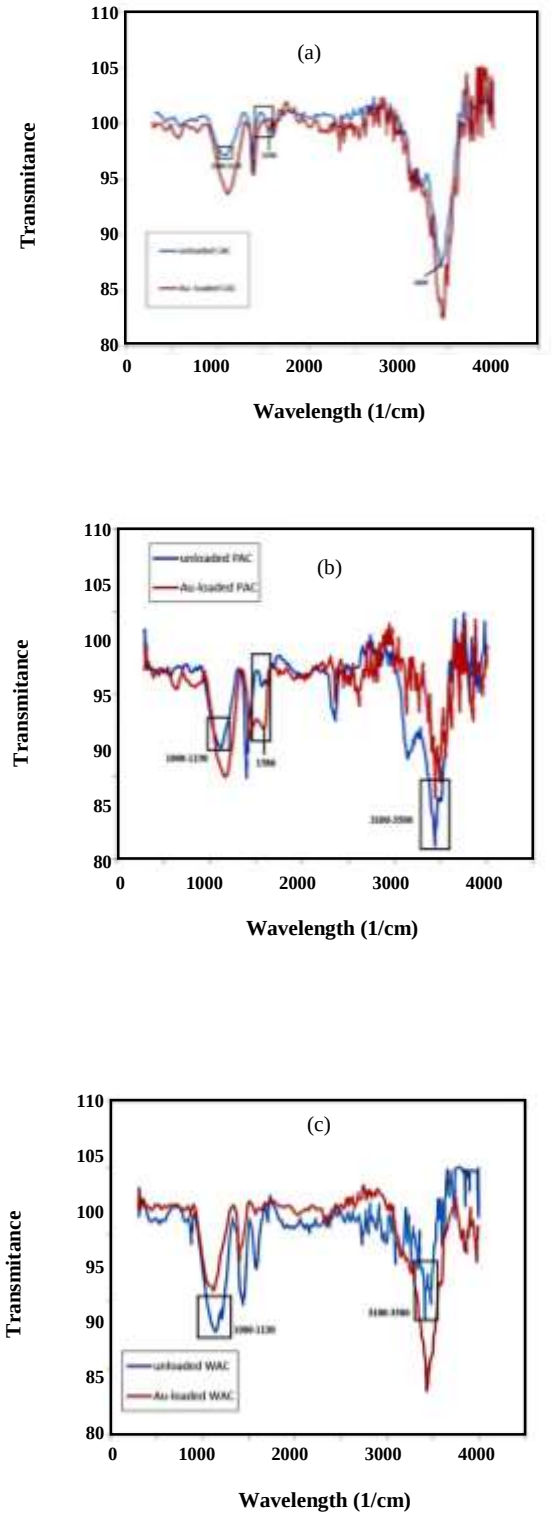

Fig. 1: FT-IR spectra of the adsorbents: CAC (a), PAC (b) and WAC (c).

Wet-Bed Compaction Hardness (WBCH)

Based on the authors' knowledge, this method has not been referenced elsewhere. This is an innovative test and defined for measuring the mechanical compaction resistance of the wet bed against hydrostatic pressure. This is an important property for the adsorption beds when applied in dynamic or column mode.

The WBCH test applied for comparing mechanical resistance of different ACs against compaction in the wet bed condition includes a graduated cylinder (2.2 cm internal diameter and 24 cm height), piston and weights. For performing each test, the same amount of the adsorbent (10g) is loaded in the cylinder. Afterwards, the wet AC is pressurized by the piston and weights (30kg) at the top of it. Bed length changes after 48 h were measured. The results are reported in the last raw of the Table 1. According to the results, CAC recorded the least bed height lost among all the tested ACs. PAC and WAC tabulated the subsequent places. The current outcome is in tune with the reported attrition hardness for the ACs (Table 1).

SEM

The SEM images of the ACs with various magnifications are shown in Fig. 2. Image J software was applied for analyzing the SEM micrographs. Pore size distribution plots and corresponding results for each adsorbent are depicted in Fig. 3 and Table 2, respectively.

As can be seen, CAC has the least value of average pore diameter. The lower pore diameter results in higher surface area which is in accordance with the values of S_{BET} reported in Table 1. The calculated values of the standard deviation in Table 2 demonstrates semi-homogeneous dispersion and consequently more favorable pore size distribution of CAC in comparison to the other ACs. Thus, the favorability of the porous structure according to the SEM analysis results is as follows: CAC > PAC > WAC

Isotherms

The Langmuir and Freundlich adsorption isotherms were applied to fit the adsorption equilibrium data of CAC, PAC and WAC. Results are shown in Fig. 4(a). The Temkin and D-R isotherms were the two more models used for the curve fitting as depicted in Fig. 4(b). Constants, correlation coefficients (R^2) and HYBRID values obtained from the curve fitting of the isotherm models are listed in Table 3.

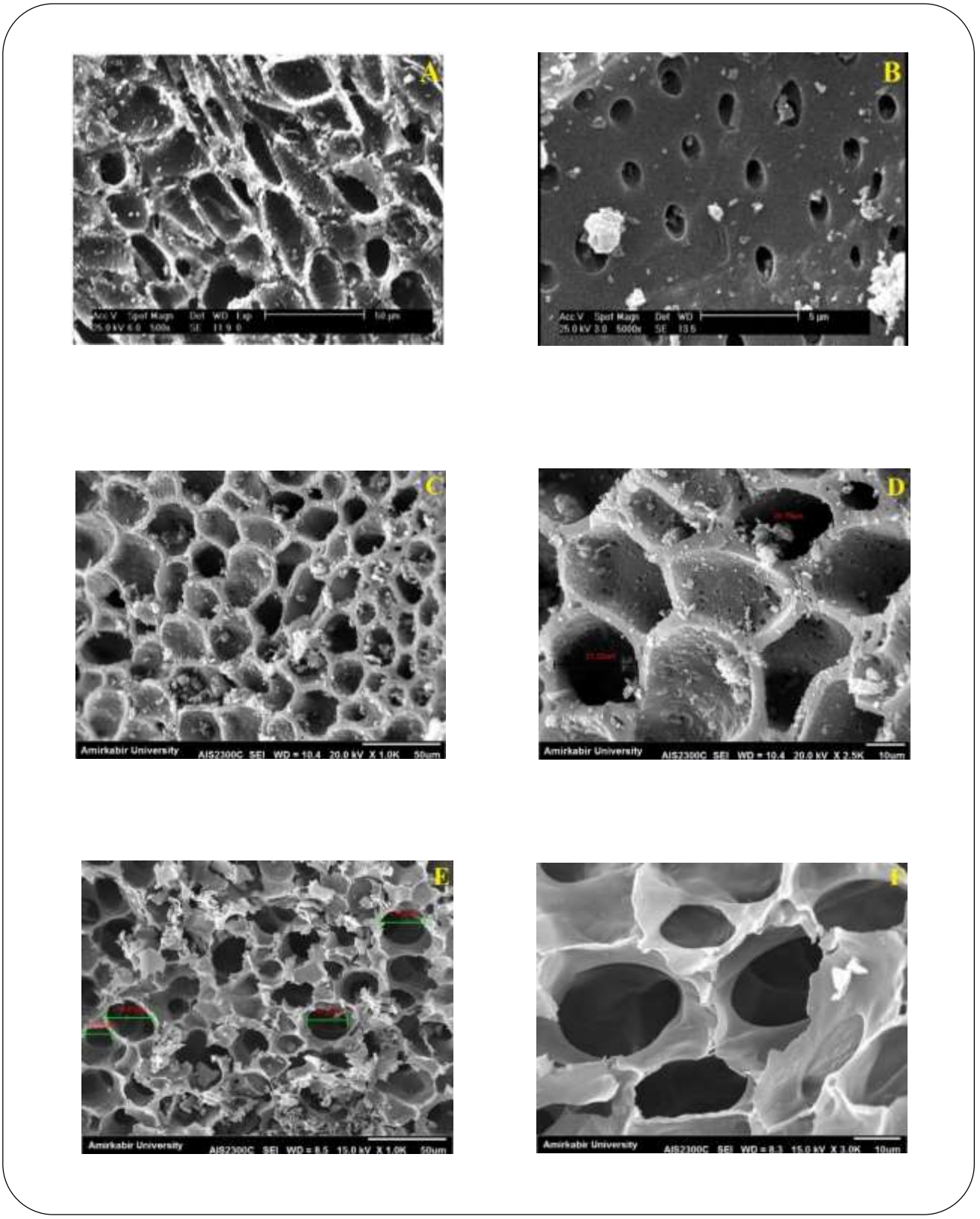

Fig. 2: SEM images of the adsorbents: CAC (A [500x], B [5000x]), PAC (C [1000x], D [2500x]) and WAC (E [1000x], F [3000x]).

Table 2: SEM image analyzing parameters for the adsorbents porous structure.

Parameter	Adsorbents		
	CAC	PAC	WAC
Average pore diameter (μm)	17.61	18.56	21.20
Standard deviation of pore size	4.38	6.52	6.73
Total number of pores per scanned surface unit (mm^{-2})	2200.23	1613.84	1344.42

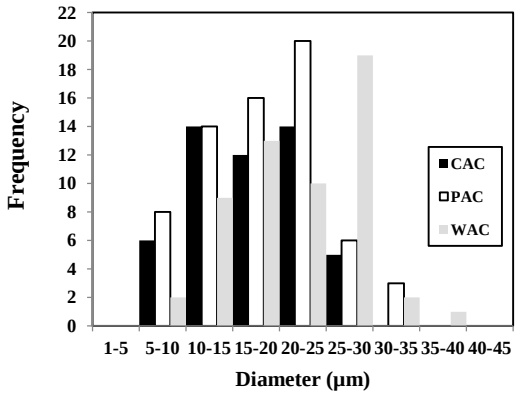

Fig. 3: Pore size distribution for the adsorbents.

According to the results, the Freundlich model provides the best fit to the equilibrium data for both CAC and PAC, as obtained by other researchers [13, 14]. This is concluded from the minimum values of HYBRID and maxium values of R^2. According to the isotherm hypotheses, some features such as multilayer coverage of adsorbates, heterogeneity of reactive sites and nonuniformity of energy distribution on the surface of AC are ascertained [31]. In the case of WAC, the highest and the lowest values of R^2 and HYBRID belong to the Freundlich and Temkin models, respectively. Parameter N (Table 3) represents values larger than unity which indicates that the type of the adsorption is physical. CAC exhibits the most adsorption capacity (q_{max}) which can be attributed to the higher intensity of OH stretching vibration and further BET surface area compared to the other ACs. The larger Langmuir constant (K_L) of PAC indicates the higher surface energy and affinity toward the adsorbate. Because R_L values obtained for all the adsorbents (Table 3) at initial concentration of 100 mg/L are below than unity, it is concluded that the adsorption is favorable.

The Temkin model assumes the adsorption heat of the molecules would decrease linearly with the surface coverage [32, 33]. The values of R^2 for the Temkin model are acceptable but not as good as those obtained for the Freundlich model. So, it is more presumable that the ACs follows nonlinear energy distribution rather than linear one. $1/b_T$ parameter of the Temkin equation represents the potential of the adsorbents for gold complex chelation. According to the data presented in Table 3, CAC introduces the most affinity toward gold cyanide among the other ACs. In addition, positive values of b_T signify that the adsorption process is exothermic [33].

D-R model introduces the lowest correlation coefficient in comparison to the other models. The highest value of *E* is belonged to CAC. As the E value for all three adsorbents is less than 8kJ/mol, the physical and multilayer adsorption nature of $Au(CN)_2^-$ on the ACs can be inferred [34]. This result is in tune with what obtained in relation to the Freundlich model. In addition, the high values of the parameter *B* (Table 3), the porosity factor, confirms the concept of the physical sorption as outlined by the other isotherm models [34].

The Gibbs free energy change (ΔG^0) is a thermodynamic parameter which can be calculated by the Van't Hoff equation:

$$\Delta G^0 = -RT\ln k_L \qquad (25)$$

Where *T* is the absolute temperature (*K*), *R* is the universal gas constant (8.314 J/mol.K) and k_L is the thermodynamic equilibrium constant estimated by the Langmuir isotherm rate constant. Negative values of ΔG^0 for all the ACs (Table 3) confirm the spontaneity of the adsorption. Obtained amounts of ΔG^0 for all three ACs (less than 40 kJ/mol) is another verification to the fact that the physisorption is occurred [35, 36].

Kinetics

A series of kinetic models were applied to describe the adsorption rate of $Au(CN)_{2(aq)}^-$ on various ACs. These models include the pseudo-first order, pseudo-second

Table 3: Isotherm parameters for gold adsorption on CAC, PAC and WAC.

Isotherm	Parameters	Adsorbent		
		CAC	PAC	WAC
Langmuir	q_{max}	40.80	32.97	23.12
	K_L	0.123	0.140	0.073
	R_L	0.075	0.066	0.120
	R^2	0.962	0.938	0.950
	ΔG^0(kJ/mol)	-11.92	-12.24	-10.63
	HYBRID	32.278	40.498	20.555
Freundlich	K_f	8.067	7.543	4.340
	N	2.556	2.888	2.870
	R^2	0.992	0.987	0.950
	HYBRID	7.784	10. 177	23.411
Temkin	A	1.471	1.766	0.710
	b_T	300.1	385.0	502.3
	R^2	0.968	0.947	0.910
	HYBRID	20.481	22.015	19.768
D-R	q_{max}	30.37	26.19	19.06
	E(kJ/mol)	0.537	0.518	0.196
	B($\times 10^6$)	1.732	1.858	12.910
	R^2	0.830	0.810	0.860
	HYBRID	199.075	166.105	53.632

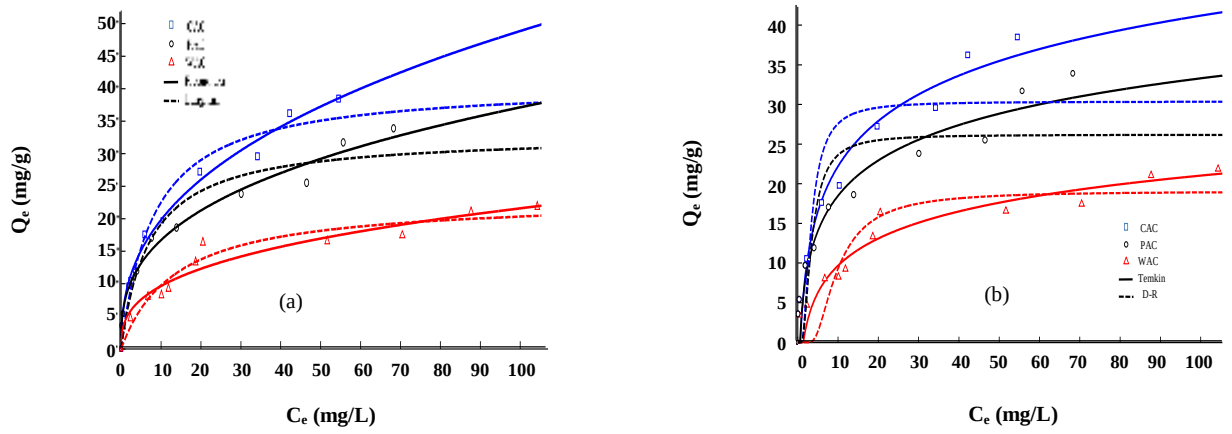

Fig. 4: Isotherm models for gold adsorption on the ACs.

Table 4: Kinetic parameters of Pseudo-first-order (PFO) and Pseudo-second-order (PSO) models for gold adsorption on CAC, PAC and WAC.

		Adsorbent		
		CAC	PAC	WAC
PFO	Model-calc. q_e	9.358	9.088	7.027
	K_1 (h^{-1})	0.95	1.14	0.64
	R^2	0.996	0.995	0.995
	HYBRID	0.952	1.047	0.987
PSO	Model-calc. q_e	10.89	10.3	8.76
	K_2 ($mg.g^{-1}.h^{-1}$)	0.112	0.16	0.076
	R^2	0.999	0.999	0.997
	HYBRID	0.023	0.255	0.392

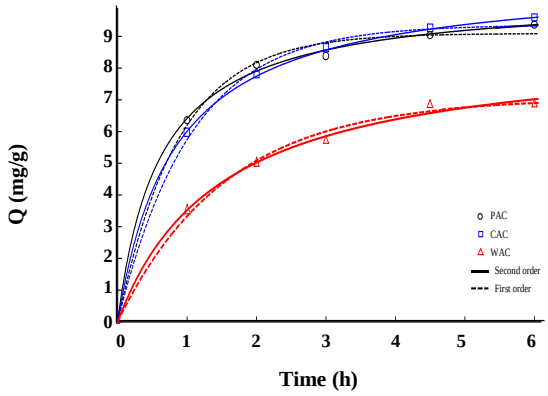

Fig. 5: The adsorbed amount of gold as a function of time onto the adsorbents.

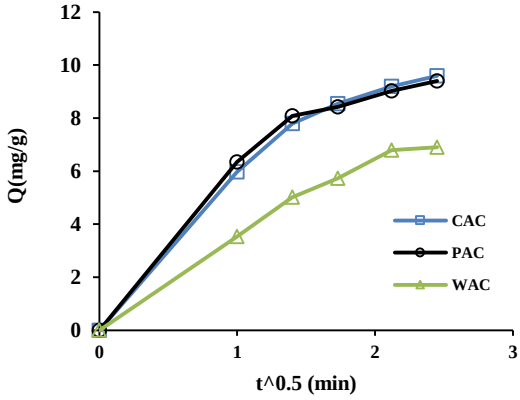

Fig. 6: Intraparticle-diffusion plots for adsorption of gold on the ACs.

order and intraparticle diffusion kinetic models. Fig. 5 shows the adsorbed amount of gold complex on different ACs as a function of time.

As can be seen, equilibrium (or adsorption capacity) for PAC occurs earlier than the other two ACs. In order to compare the kinetic characteristics of the activated carbons, the constant parameters, regression coefficients and HYBRID values are reported in Table 4. Both of the kinetic models suggest high correlation coefficients and favorable agreement between the q_t values calculated from the models and those obtained from the experiments; however, lower HYBRID values indicates that the psudo-second order model is of higher appropriateness. This leads to select the pseudo-second order model for representing the sorption kinetics.

Higher uptake rate constant (k_2) belongs to PAC which verifies the superior adsorption rate of the gold complex onto PAC.

The plots of q_t versus $t^{0.5}$ for gold adsorption on different adsorbents (Fig.6) are nonlinear. Therefore, it is concluded that the intraparticle diffusion is not the sole rate-controlling mechanism of the adsorption.

Fixed-bed column study

Column data analysis

The breakthrough curves obtained for the ACs at two

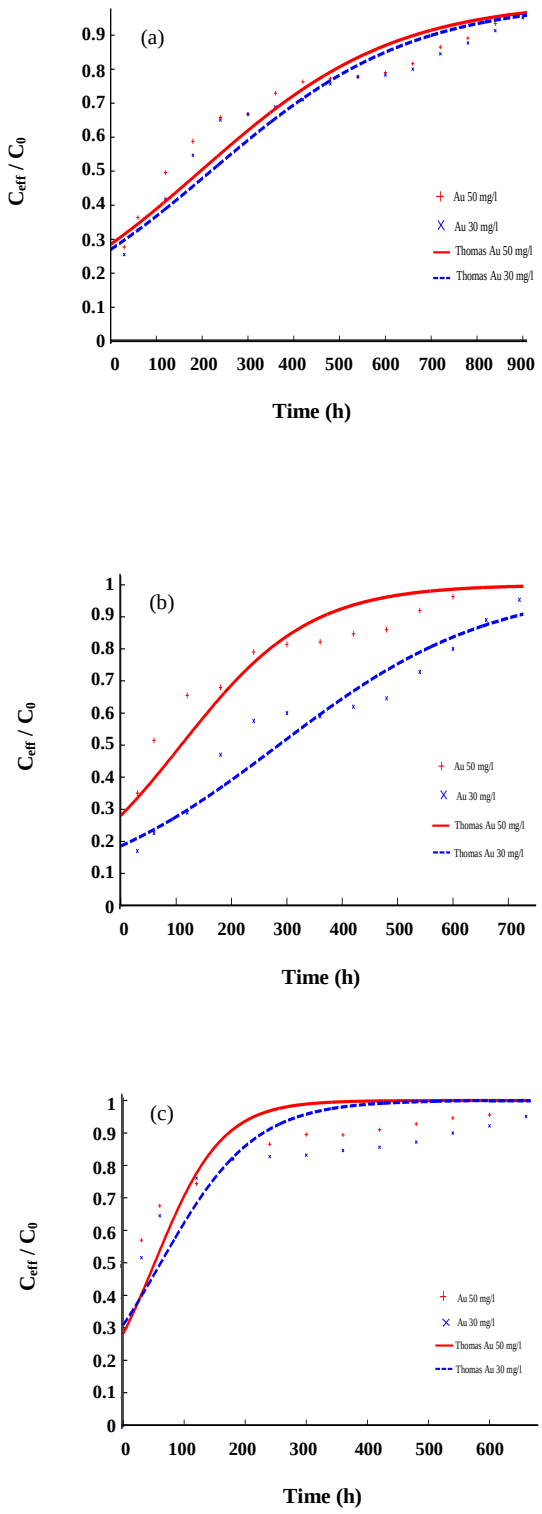

Fig. 7: Effect of initial concentration on gold removal by CAC (a), PAC (b) and WAC (c).

different gold inlet concentrations (30 and 50 mg/L) are shown in Fig.7. Adsorption parameters, calculated according to the mathematical framework, are presented in Table 5. As can be concluded from both Fig.7 and Table 5, higher feed concentration results in faster breakthrough time (t_b) and steeper slope of the breakthrough curve. As it is obvious from Fig. 7, for all the adsorbents (especially PAC and WAC) with 50 mg/l $Au(CN)^-_{2(aq)}$ as the feed, the adsorption rate is initially high and after sometimes decreases by reducing the removal efficiency of the system and finally meets a constant at the equilibrium time, t=600 and t=300 min for PAC and WAC, respectively. At the lower influent concentration (30 mg/l), after the mentioned times, the adsorbents are still unsaturated and able to receive more inlet solution. In other words, higher feed concentration results in faster bed saturation and consequently faster completion of the breakthrough time.

According to the literature, the performance of the breakthrough curves is less affected by the feed concentration when heavy metals are the adsorbing components [37]. The insignificant effect of the feed concentration on the adsorbents performances (Fig.8) may be also attributed to unremarkable amounts of bed adsorption capacity (q_0 values in Thomas model). Moreover, there is not sufficient concentration driving force in the system when feed is a dilute solution. Therefore, breakthrough curves characteristics are not highly affected by the feed concentration.

It is noticeable that PAC, at both concentrations, shows the highest value of t_b. This means that better utilization of the bed adsorption capacity is possible for this activated carbon. This may be attributed to better adsorption kinetic of PAC compared to the other ACs.

For all the breakthrough curves, Mass Transfer Zone (MTZ) lies between C/C_0 = 0.05 to C/C_0 = 0.95. Considering constant operating conditions such as type of the adsorbent used, the initial concentration of influent and the residence time, the higher values of t_b (longer breakthrough time) results in the lower values of MTZ. This reduction in the length of MTZ reflects better utilization of the adsorption capacity of the bed in the adsorption process.

Increasing the gold concentration in the influent provides higher driving force for mass transfer, so the adsorbents saturation occurs more rapidly. This results in a decrease in the exhaust time (t_e) and the treated volume (V_{eff}).

Table 5: Breakthrough results for the column adsorption experiments.

Adsorbent	C_0(mg/L)	Q(mL/min)	t_b(min)	t_e(h)	V_{eff}(mL)	q_{total}(mg)	m_{total}(mg)	q_{eq}(mg/g)	C_{eq}(mg/l)	Y(%)
CAC	50	20	6.0	14.5	17400	262.88	864	37.55	34.54	30.42
	30	20	9.6	15	18000	163.74	540	23.40	20.9	30.32
PAC	50	20	7.8	10.6	13200	157.11	660	22.44	38.09	23.80
	30	20	13.2	12.0	14400	181.74	432	25.96	17.38	42.06
WAC	50	20	4.2	9.6	12000	120.77	600	17.25	39.9	20.12
	30	20	7.2	11.0	13200	76.77	396	10.96	24.18	19.38

As expected, for each investigated concentration, the least and the greatest values of both t_e and V_{eff} belongs to WAC and CAC, respectively. By increasing the influent concentration for the adsorbents the equilibrium gold adsorption (q_{eq}) increases. This may be attributed to the higher driving force for the adsorption which provides better conditions for overcoming the mass transfer resistances [38]. At concentration of 50mg/l, the maximum value of q_{total} belongs to CAC and the minimum value belongs to WAC. This result matches the higher value of q_{max} mentioned in the isothermal study. At lower feed concentration (30mg/l), PAC shows the highest adsorption capacity which is possibly attributed to the faster uptake rate. Similar scenario takes place for total removal percentage (Y) meaning that CAC have the best removal percentage at higher concentration of 50 mg/l. It is obvious from the results that the kinetic of adsorption plays more crucial role at dilute concentrations. On the other hand, the adsorption capacity of the ACs is of more practical importance for determining the column characteristics at higher feed concentrations. The unadsorbed gold at the equilibrium (C_{eq}) for all the adsorbents is also found to be increased with increasing the inlet concentration. This is related to the faster saturation of adsorption sites at higher concentrations. It is worth mentioning that the 'S-type' profile is usually obtained for adsorbates with small molecular diameters and simple structures [39]. Thus, this shape is not expected for the complex of $Au(CN)_{2(aq)}^{-}$.

Breakthrough curve modeling

Thomas model

The experimental data were fitted to the Thomas model using nonlinear regression method. The estimated parameters of the Thomas equation, the correlation coefficients are given in Table 6. In all the cases, the value of k_{Th} decreases with increasing the inlet gold concentration because of an increase in the mass transport resistance [25, 40]. Therefore, increasing the gold concentration enhances the mass transfer driving force and results in larger amounts of q_0. As before, at upper concentration of 50 mg/l, CAC is the best adsorbent due to higher q_0 values; however, at lower concentration (30 mg/L) PAC exhibits better performance.

There is no clear-cut relationship between feed concentration, k_{Th} and maximum adsorption capacity of the bed (q_0 or q_{eq}) based on the literature. Different scenarios can be observed as follows:

- Increased values of both k_{Th} and q_0 [41]
- Decreased values of both k_{Th} and q_0 [42]
- Increased k_{Th} values and decreased q_0 values [43]
- Decreased k_{Th} values and increased q_0 values [25,40]

In our case study, increased inlet concentration decreases the k_{Th} but increases the q_0 by enhancement of the concentration driving force. It is worthy of notice that k_{th} is a kinetic parameter; however, q_0 is a dynamic equilibrium one. Therefore, there is no direct connection between the two.

Yoon-Nelson model

For each tested adsorbent the parameters τ, k_{YN} and R^2 obtained using nonlinear regression are listed in Table 6. As can be seen, the value of τ decreases with increasing the gold concentration. This indicates that the saturation of the bed is occurred faster [44] and the length of the adsorption zone decreased with increasing the feed concentration [45].

Table 6: Parameters of the column models for gold-cyanide adsorption on different activated carbons.

	Operating conditions			Thomas parameters				Yoon–Nelson parameters				Adams–Bohart parameters			
Adsorption	Q(mL/min)	m(g)	C_0(mg/l)	K_{TH}(mL/min.mg) $\times 10^{-5}$	q_0(mg/g) $\times 10^4$	R^2	HYBRID	K_{YN}(min^{-1}) $\times 10^{-3}$	τ(min)	R^2	HYBRID	K_{AB}(l/min.mg) $\times 10^{-5}$	N_0(mg/L) $\times 10^4$	R^2	HYBRID
CAC	20	7	50	9.04	2.913	0.866	0.6571	4.69	195.4	0.866	0.6	1.625	5.665	0.686	1.978
	20	7	30	13.40	2.128	0.882	0.9928	4.55	222.8	0.882	0.68	3.226	3.321	0.742	2.27
PAC	20	7	50	17.52	1.50	0.836	0.9231	8.40	109.5	0.836	0.91	2.782	3.209	0.631	1.9
	20	7	30	18.54	2.281	0.912	1.054	5.19	285.2	0.912	0.97	6.086	2.367	0.839	2.24
WAC	20	7	50	36.25	0.7384	0.769	1.573	18.13	51.68	0.769	1.56	2.196	3.053	0.489	1.61
	20	7	30	43.69	0.5287	0.702	1.78	13.09	61.69	0.702	1.7	3.453	2.024	0.478	1.66

Adams-Bohart model

Using nonlinear regression analysis, the relative constants and correlation coefficients for all the three adsorbents were calculated and the results are reported in Table 6. The saturation concentration of gold (N_0) is enhanced with an increase in the influent concentration due to the higher loading of adsorbate on the bed. As expected, the maximum and minimum values of N_0 for both tested concentration belongs to CAC and WAC, respectively. The K_{AB} values decreases with increasing the gold concentration in the feed. This fact indicates that the kinetics of the overall system is mainly affected by the external mass transfer at the initial part of the adsorption column [25].

A comparison among R^2 values obtained for all the three models reveals that both the *Thomas* and *Yoon-Nelson* provide appropriate fit in comparison to the Adams-Bohart model under the same experimental conditions. Considering the highest R^2 and the lowest HYBRID values, the Yoon-Nelson is the best model for the dynamic modeling of the AC/gold adsorption system. Similar results have been obtained by other researchers [38, 46]. So, it can be said that the adsorption process is not dominated by the surface diffusion mechanism.

Fig. 8 represents the breakthrough curves for gold adsorption by various adsorbents at the same operating condition. The breakthrough curve for gold adsorption onto CAC is less steep than the curves of the other adsorbents. After 600 min of continuous flow, both PAC and WAC curves experience exhaustion, while CAC does not. Thus, it is inferred that the favorability of the column adsorption by the ACs follows this order: CAC > PAC > WAC

CONCLUSIONS

Gold adsorption from gold-cyanide leach solution onto three types of activated carbons with different precursors including walnut shell, peach stone, and coconut shell was investigated in both batch and fixed-bed column adsorption conditions. Characterization of the adsorbents was performed using FTIR, BET, SEM and WBCH tests and CAC suggested superior specifications such as surface area (2200 m^2/g), chemistry and hardness values (% 99 and 1.3 cm). The Freundlich isotherm was well fitted to the equilibrium adsorption data and CAC recorded the highest adsorption capacity around 41 mg/g. Pseudo-second-order model provides better description of the kinetic data with the higher adsorption rate constant ascribed to PAC. In the fixed-bed column study, higher gold inlet concentrations resulted in faster bed saturation, steeper breakthrough curves and higher bed adsorption capacity. According to the results, CAC introduced better performance in both batch and continuous adsorption modes. With considering the economic considerations and the availability of the starting materials for the production of activated carbon in our country, peach stone AC is demonstrated to be a potential alternative to the coconut shell-based AC for applying in gold extraction process.

Acknowledgments

The authors gratefully thank Zar Kuh Mining Company (Qorveh, Kurdistan, Iran) for their support during completion of this project.

Nomenclature

A	Temkin isotherm constant, l/g
AC	Activated carbon

A_r	The cross-sectional area of the bed, cm^2
B	D–R constant related to mean free energy of adsorption, mol^2/J^2
b_T	Temkin isotherm constant relating to heat of adsorption, J/mol
C_{ad}	The concentration of gold removal, mg/L
C_0	Initial concentration, mg/L
C_e	Equilibrium concentration, mg/L
C_{eff}	Outlet gold concentration, mg/L
C_{eq}	Unabsorbed gold concentration, mg/L
C_t	Concentration at time t, mg/L
E	Adsorption energy, kJ/mol
k_f	Freundlich constant $(mg/g)\ (l/g)^{1/n}$
k_L	Langmuir isotherm constant, l/mg
k_1	Pseudo first-order rate constant, min^{-1}
k_2	Pseudo second-order rate constant, g/mg min
k_p	Intraparticle diffusion kinetic model constant, $mg/g\ min^{0.5}$
k_{AB}	The kinetic constant, l/mg min
k_{Th}	The Thomas model constant, mL/min mg
k_{YN}	The rate constant, min^{-1}
m	Mass of the adsorbent, g
m_{total}	Total amount of gold sent to column, mg
1/n	Freundlich exponent
N_0	The saturation concentration, mg/L
q_0	The adsorption capacity, mg/g
q_e	Equilibrium gold uptake, mg/g
q_{eq}	Maximum capacity of the column, mg/g
q_{max}	Monolayer sorption capacity, mg/g
q_t	Adsorption capacity at any time t, mg/g
q_{total}	The total mass of gold adsorbed, mg
Q	The volumetric flow rate, cm^3/min
R^2	Correlation coefficient
R	Gas constant, kJ/ kg mol K
R_L	Separation factor
t	The total flow time, min
t_b	Break through time, min
t_e	Bed exhaustion time, h
t_{total}	The total flow time, min
T	Temperature, K
U_0	The superficial velocity, cm/min
V	Volume of adsorbate solution, L
V_{eff}	The effluent volume, mL
Z	The bed depth of the fix-bed column, cm
Y	The removal percent of gold ions, %

Greek symbol

τ	The time required for 50% adsorbate breakthrough, min
ε	Polanyi potential
ΔG^0	Free energy changes, kJ/mol

Received : Oct. 14, 2018 ; Accepted :Jan. 28, 2019

REFERENCES

[1] Prasad M.S., Mensah-Biney R., Pizarro R.S., Modern Trends in Gold Processing—Overview, *Miner. Eng.*, **4**(12):1257-77(1991).

[2] Kondos P.D., Deschênes G., Morrison R.M., Process Optimization Studies in Gold Cyanidation, *Hydrometallurgy*, 39(1-3):235-50(1995).

[3] Lu Y., Song Q., Xu Z., Integrated Technology for Recovering Au from Waste Memory Module by Chlorination Process: Selective Leaching, Extraction, and Distillation, *J. Cleaner Production.*, **161**: 30-39 (2017).

[4] McDougall G.J., Hancock R.D., Gold Complexes and Activated Carbon, *Gold Bulletin*, **14**(4): 138-153 (1981).

[5] Seke MD, Sandenbergh RF, Vegter NM, Effects of the Textural and Surface Properties of Activated Carbon on the Adsorption of Gold di-Cyanide, *Miner. Eng.*, **13**(5): 527-540(2000).

[6] Navarro P, Vargas C, Efecto de Las Propiedades Físicas del Carbón Activado en la Adsorción de Oro Desde Medio Cianuro, *Revista de Metalurgia*, **46**(3): 227-39(2010).

[7] Ladeira A.C., Figueira M.E., Ciminelli V.S., Characterization of Activated Carbons Utilized in the Gold Industry: Physical and Chemical Properties, and Kinetic Study, *Miner. Eng.*, **6**(6):585-96(1993).

[8] Gupta N., Balomajumder C., Agarwal V.K., Adsorption of Cyanide Ion on Pressmud Surface: A Modeling Approach, *Chem. Eng. J.*, **191**: 548-56 (2012).

[9] Soleimani M., Kaghazchi T., Adsorption of Gold Ions from Industrial Wastewater Using Activated Carbon Derived from Hard Shell of Apricot Stones –An Agricultural Waste, *Bioresour. Technol.*, **99**(13): 5374-5383 (2008).

[10] Ahmadpour A., Do D.D., The Preparation of Activated Carbon from Macadamia Nutshell by Chemical Activation, *Carbon*, **35**(12): 1723-32 (1997).

[11] Toles C.A., Marshall W.E., Johns M.M., Granular Activated Carbons from Nutshells for the Uptake of Metals and Organic Compounds, *Carbon*, **35**(9): 1407-1414 (1997).

[12] Aygün A., Yenisoy-Karakaş S., Duman I., Production of Granular Activated Carbon from Fruit Stones and Nutshells and Evaluation of Their Physical, Chemical and Adsorption Properties, *Micropor. Mesopor. Mater.*, **66**(2-3): 189-195 (2003).

[13] Soleimani M., Kaghazchi T., Activated Hard Shell of Apricot Stones: A Promising Adsorbent in Gold Recovery, *Chin. J. Chem. Eng.*, **16**(1):112-118 (2008).

[14] Yalcin M., Arol A.I., Gold Cyanide Adsorption Characteristics of Activated Carbon of Non-Coconut Shell Origin, *Hydrometallurgy*, **63**(2):201-206 (2002).

[15] Ramírez-Muñiz K., Song S., Berber-Mendoza S., Tong S., Adsorption of the Complex Ion Au (CN) 2-onto Sulfur-Impregnated Activated Carbon in Aqueous Solutions, *J. Colloid Interface Sci.*, **349**(2): 602-606 (2010).

[16] Poinern G.E., Senanayake G., Shah N., Thi-Le X.N., Parkinson G.M., Fawcett D., Adsorption of the Aurocyanide, $Au(CN)_2$-Complex on Granular Activated Carbons Derived from Macadamia Nut Shells–A Preliminary Study, *Miner. Eng.*, **24**(15): 1694-1702 (2011).

[17] Buah W.K., Williams P.T., Granular Activated Carbons from Palm Nut Shells for Gold di-Cyanide Adsorption, *Int. J. Miner. Metall. Mater.*, **20**(2):172-9(2013).

[18] Asadi-Kesheh R., Mohtashami S.A., Kaghazchi T., Asasian N., Soleimani M., Bagasse-Based Adsorbents for Gold Recovery from Aqueous Solutions, *Sep. Sci. Technol.*, **50**(2): 223-232 (2015).

[19] Vargas C, Navarro P, "Adsorption of $Au(CN)_2$ Onto Activated Carbon Impregnated with a Cationic Surfactant", *7th International Seminar on Hydrometallurgy*, (2015).

[20] Dolphen R., Sakkayawong N., Thiravetyan P., Nakbanpote W., Adsorption of Reactive Red 141 from Wastewater onto Modified Chitin, *J. Hazard. Mater.*, **145**(1-2): 250-255 (2007).

[21] Baral S.S., Das N., Ramulu T.S., Sahoo S.K., Das S.N., Chaudhury GR, Removal of Cr (VI) by thermally Activated Weed Salvinia Cucullata in a Fixed-Bed Column, *J. Hazard. Mater.*, **161**(2-3):1427-35(2009).

[22] Ahmad A.A., Hameed B.H., Fixed-Bed Adsorption of Reactive Azo Dye onto Granular Activated Carbon Prepared from Waste, *J. Hazard. Mater.*, **175**(1-3): 298-303 (2010).

[23] Yoon Y.H., NELSON J.H., Application of Gas Adsorption Kinetics I. A Theoretical Model for Respirator Cartridge Service Life, *Am. Ind. Hyg. Assoc. J.*, **45**(8): 509-516 (1984).

[24] Goel J., Kadirvelu K., Rajagopal C., Garg V.K., Removal of Lead (II) by Adsorption Using Treated Granular Activated Carbon: Batch and Column Studies, *J. Hazard. Mater.*, **125**(1-3): 211-220 (2005).

[25] Aksu Z., Gönen F., Biosorption of Phenol by Immobilized Activated Sludge in a Continuous Packed Bed: Prediction of Breakthrough Curves, *Process Biochem.*, **39**(5): 599-613(2004).

[26] Huang C.C., Li H.S., Chen C.H., Effect of Surface Acidic Oxides of Activated Carbon on Adsorption of Ammonia, *J. Hazard. Mater.*, **159**(2-3):5 23-527 (2008).

[27] Martinez M.L., Torres M.M., Guzman C.A., Maestri D.M., Preparation and Characteristics of Activated Carbon from Olive Stones and Walnut Shells, *Ind. Crops. Prod.*, **23**(1): 23-28 (2006).

[28] Abidin M.A., Jalil A.A., Triwahyono S., Adam S.H., Kamarudin N.N., Recovery of Gold (III) from an Aqueous Solution onto a Durio Zibethinus Husk, *Biochem. Eng. J.*, **54**(2):124-131(2011).

[29] Gurung M., Adhikari B.B., Kawakita H., Ohto K., Inoue K., Alam S., Recovery of Au (III) by Using Low Cost Adsorbent Prepared from Persimmon Tannin Extract, *Chem. Eng. J.*, **174**(2-3): 556-63 (2011).

[30] Lladó J., Lao-Luque C., Ruiz B., Fuente E., Solé-Sardans M., Dorado A.D., Role of Activated Carbon Properties in Atrazine and Paracetamol Adsorption Equilibrium and Kinetics, *Process Saf. Environ.*, 95:51-9(2015).

[31] Srihari V., Das A., Comparative Studies on Adsorptive Removal of Phenol by Three Agro-Based Carbons: Equilibrium and Isotherm Studies, *Ecotoxic. Environ. Saf.*, **71**(1): 274-283(2008).

[32] Hydari S., Sharififard H., Nabavinia M., Reza Parvizi M., A Comparative Investigation on Removal Performances of Commercial Activated Carbon, Chitosan Biosorbent and Chitosan/Activated Carbon Composite for Cadmium, *Chem. Eng. J.*, **193**: 276-282 (2012).

[33] Salehi E., Madaeni S.S., Rajabi L., Derakhshan A.A., Daraei S., Vatanpour V., Static and Dynamic Adsorption of Copper Ions on Chitosan/Polyvinyl Alcohol Thin Adsorptive Membranes: Combined Effect of Polyethylene Glycol and Aminated Multi-Walled Carbon Nanotubes, *Chem. Eng. J.*, **215**: 791-801 (2013).

[34] Wu X.W., Ma H.W., Li J.H., Zhang J., Li Z.H., The Synthesis of Mesoporous Aluminosilicate Using Microcline for Adsorption of Mercury (II), *J. Colloid Interface Sci.*, **315**(2):555-561(2007).

[35] Aydın H., Baysal G., Adsorption of Acid Dyes in Aqueous Solutions by Shells of Bittim (Pistacia Khinjuk Stocks), *Desalination*, **196**(1-3): 248-59 (2006).

[36] Bulut Y., Aydın H., A Kinetics and Thermodynamics Study of Methylene Blue Adsorption on Wheat Shells, *Desalination*, **194**(1-3):259-67(2006).

[37] Tovar-Gómez R, Moreno-Virgen M.R., Dena-Aguilar J.A., Hernández-Montoya V., Bonilla-Petriciolet A., Montes-Morán M.A., Modeling of Fixed-Bed Adsorption of Fluoride on Bone Char Using a Hybrid Neural Network Approach, *Chem. Eng. J.*, **228**:1098-109(2013).

[38] Chen S., Yue Q., Gao B., Li Q., Xu X., Fu K., Adsorption of Hexavalent Chromium from Aqueous Solution by Modified Corn Stalk: A Fixed-Bed Column Study, *Bioresour. Technol.*, **113**: 114-20 (2012).

[39] Walker G.M., Weatherley L.R., Adsorption of Acid Dyes on to Granular Activated Carbon in Fixed Beds, Water Res., **31**(8): 2093-2101(1997).

[40] Han R., Zhang J., Zou W., Xiao H., Shi J., Liu H., Biosorption of Copper (II) and Lead (II) from Aqueous Solution by Chaff in a Fixed-Bed Column, *J. Hazard. Mater.*, **133**(1-3): 262-8(2006).

[41] Hernandez-Eudave M.T., Bonilla-Petriciolet A., Moreno-Virgen M.R., Rojas-Mayorga C.K., Tovar-Gomez R, Design Analysis of Fixed-Bed Synergic Adsorption of Heavy Metals and Acid Blue 25 on Activated Carbon, *Desalin. Water Treat.*, **57**(21): 9824-36(2016).

[42] Yahaya N.K., Abustan I., Latiff M.F., Bello O.S., Ahmad M.A., Fixed-bed Column Study for Cu (II) Removal from Aqueous Solutions Using Rice Husk Based Activated Carbon, *Int. J. Eng. Technol.*, **11**(1): 248-252 (2011).

[43] Shahbazi A., Younesi H., Badiei A., Functionalized SBA-15 Mesoporous Silica by Melamine-Based Dendrimer Amines for Adsorptive Characteristics of Pb (II), Cu (II) and Cd (II) Heavy Metal Ions in Batch and Fixed Bed Column, *Chem. Eng. J.*, **168**(2): 505-518 (2011).

[44] Ho Y.S., McKay G., Sorption of Dye from Aqueous Solution by Peat, *Chem. Eng. J.*, **70**(2): 115-124 (1998).

[45] Goel J., Kadirvelu K., Rajagopal C., Garg V.K., Removal of Lead (II) by Adsorption Using Treated Granular Activated Carbon: Batch and Column Studies, *J. Hazard. Mater.*, **125**(1-3): 211-220 (2005).

[46] Nazari G., Abolghasemi H., Esmaieli M., Pouya E.S., Aqueous Phase Adsorption of Cephalexin by Walnut Shell-Based Activated Carbon: A Fixed-Bed Column Study, *Appl. Surf. Sci.*, **375**:144-153 (2016).